

Schulte-Pelkum, V., et al., 2019, Mantle earthquakes in the Himalayan collision zone: *Geology*, <https://doi.org/10.1130/G46378.1>

Supplementary information

The supplementary information consists of four figures and a table. Fig. DR1 contains information on event statistics in the original event set of ~500. Fig. DR2 contains similar catalog information for the event set selected for S-P analysis by station distance, location error, and pick uncertainty as well as choice of the location error and pick uncertainty cutoffs. Fig. DR3 is an S-P profile showing events applying only the station distance cutoff and not the location error and pick uncertainty cutoffs. Fig. DR4 shows raw waveforms and picks for all deep events in southern Tibet (numbered events in Fig. 2C, Fig. 4).

Table DR1 lists the locations and origin times for those 6 events. To construct the previously relocated and published ~500 event set, earthquakes were initially located with 1-D velocity models (Monsalve et al., 2006); subsequently, a 2D velocity model was determined for the region (Monsalve et al., 2008), and that model was used for a probabilistic non-linear earthquake location algorithm (Lomax, 2004) with results published in Monsalve et al. (2009). The epicentral location error refers to the misfit after the probabilistic non-linear location.

The larger magnitude deep events shown in the inset map in Fig. 1 were compiled by Chen and Yang (2004) and were taken from Table S1 in that publication's supplementary information. For the three events within our study area, the detailed analysis is from Ekstrom (1987) and Chen (1988) for the 1986 event T8; Chen and Kao (1996) for the 1988 event T9 (see also Ghimire and Kasahara, 2007, cited in main text); and Zhu and Helmberger (1996) for the 1992 event T12. Body wave magnitudes for these three events are $m_b = 4.9, 5.5,$ and 6.4 (Fig. 1). They are located near or within deep microseismic event clusters A, B, and C (Fig. 1). For the magnitude range of the three larger deep events, Omori's law for aftershock decay (Utsu et al., 1995) predicts a rapid falloff in aftershock magnitude within days to months after the mainshock. Sustained activity with magnitudes of $M_L = 2$ to 3 (Fig. DR2) decades after the larger event therefore does not match characteristics of aftershocks. The geographical extent of the clusters A-C also far exceeds the possible fault dimensions of earthquakes in the $4.9 - 6.5$ magnitude range.

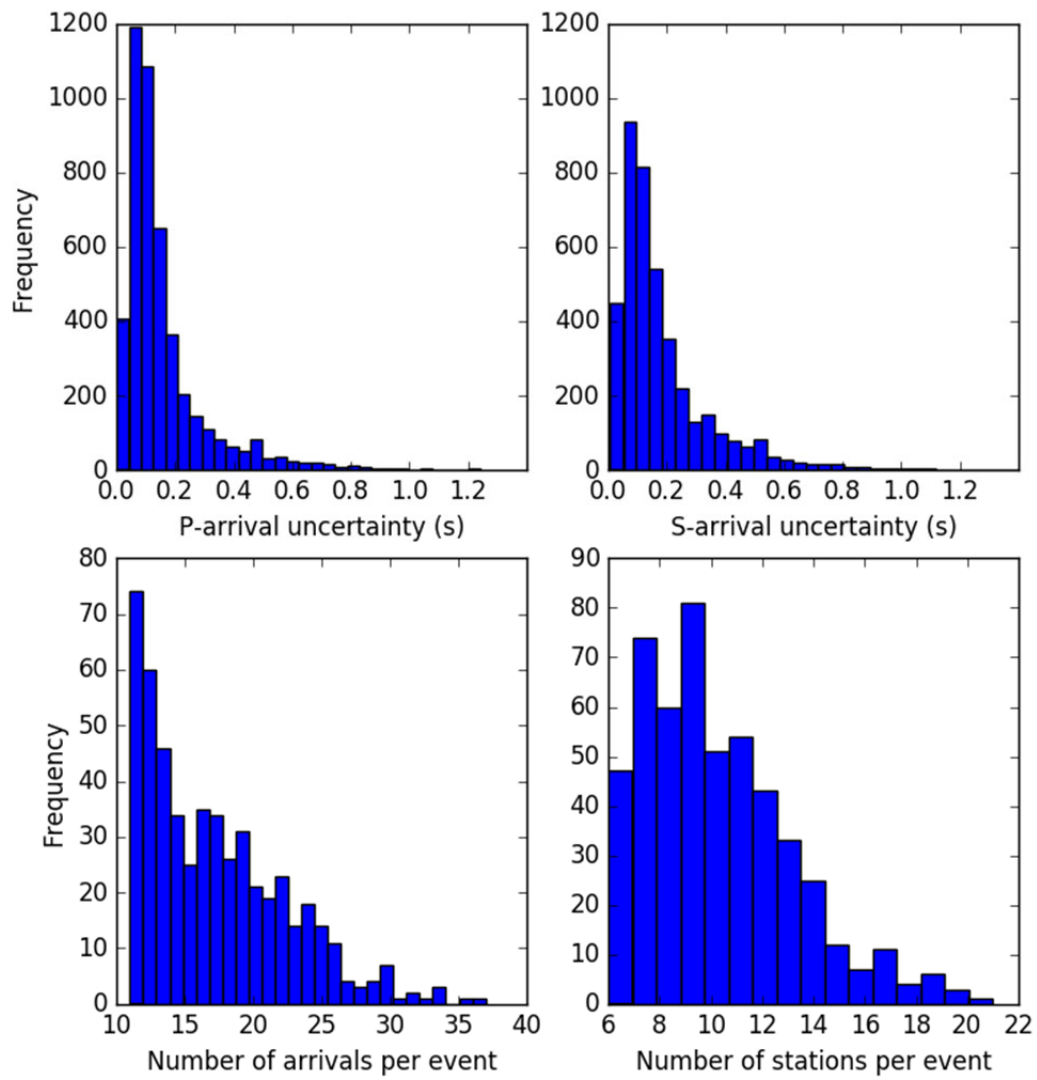


Figure DR1. Pick statistics for the initial ~500 event set.

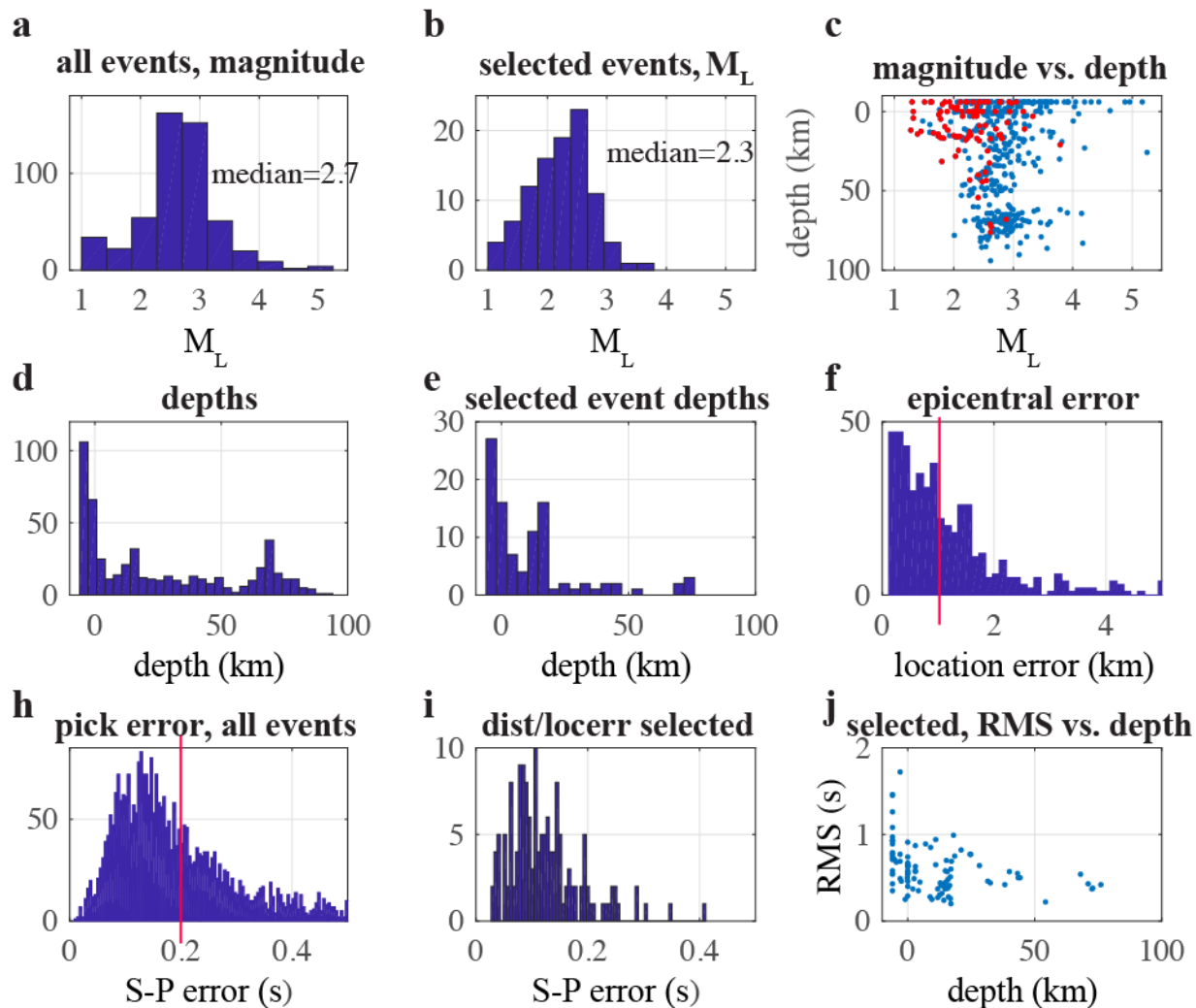


Figure DR2. Statistics for the initial and selected event set. Selected event set has < 35 km station to event distance, pick uncertainty < 0.2 s, epicentral location error < 1 km. (a) Histogram of local magnitude for all events. (b) Histogram of local magnitude for selected event set. (c) Local magnitude vs. event depth for all (blue) and selected (red) events. (d) Depth distribution for all events. (e) Depth distribution for selected events. (f) Epicentral location error distribution for all events. Red line marks approximate half-amplitude width chosen as a cutoff for selected event set. (h) S-P pick uncertainty distribution for all events. Red line marks approximate half-amplitude width chosen as a cutoff for selected event set. (i) Distribution of S-P uncertainty for events after selection by station distance and location error cutoff, but before applying pick uncertainty cutoff. (j) Pick time RMS misfit remaining after relocation for selected event set shown as a function of event depth.

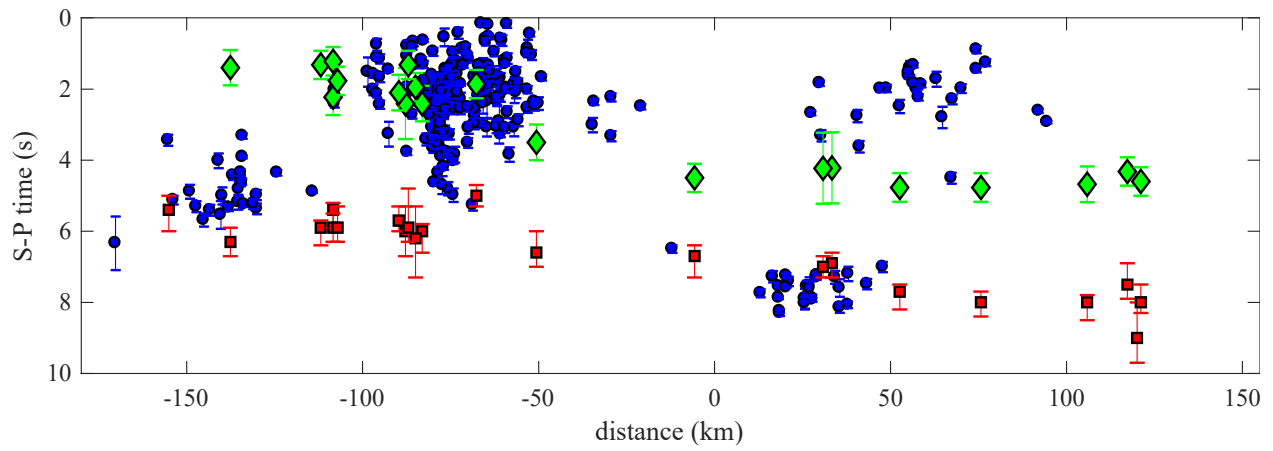
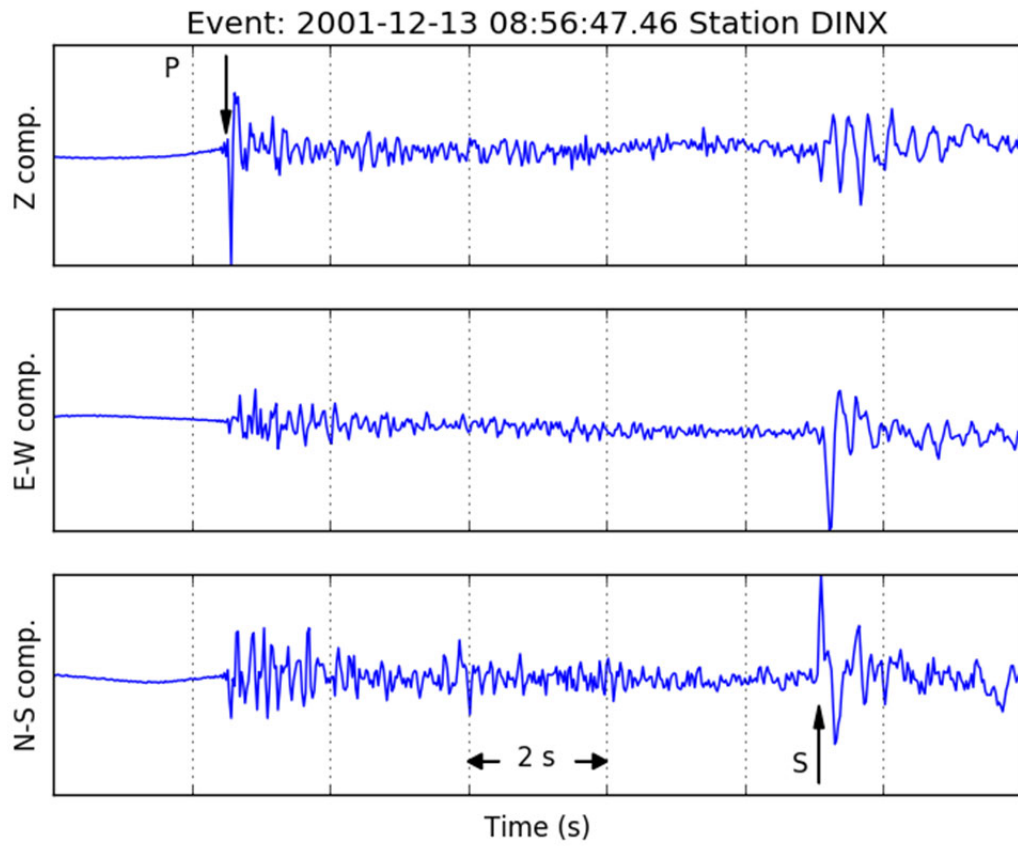
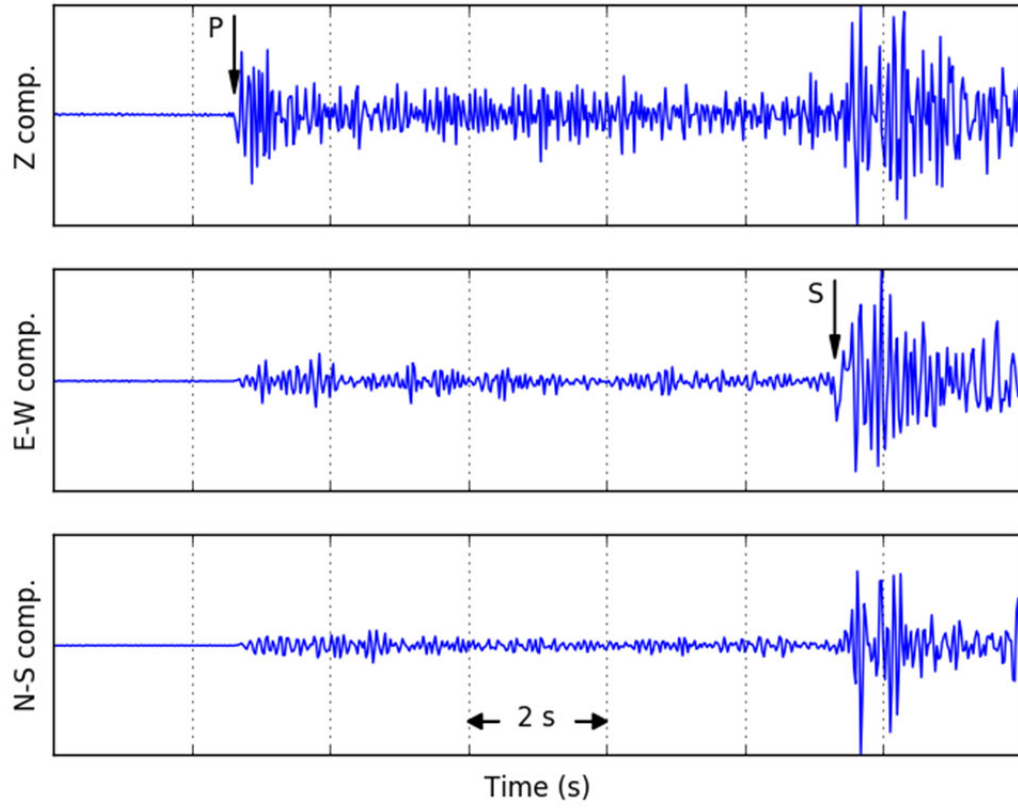


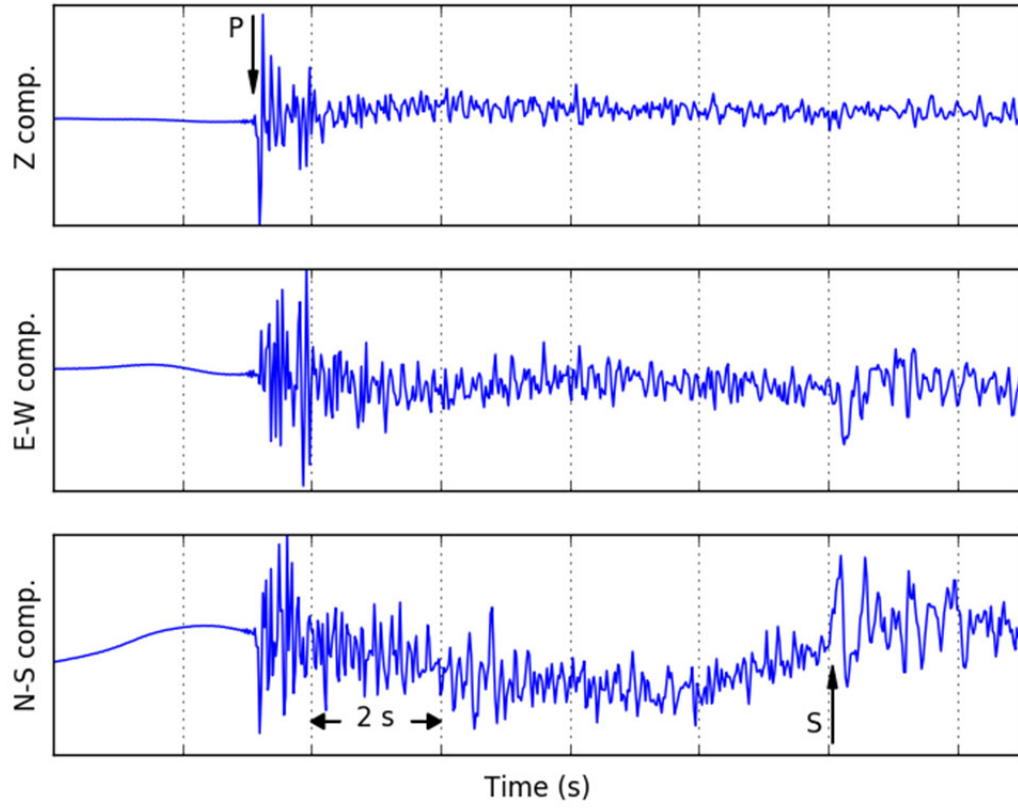
Figure DR3. As in Fig. 2C, but with relaxed station distance criterion (40 km maximum event-station distance) and no location error and pick uncertainty cutoffs applied to the initial event set.



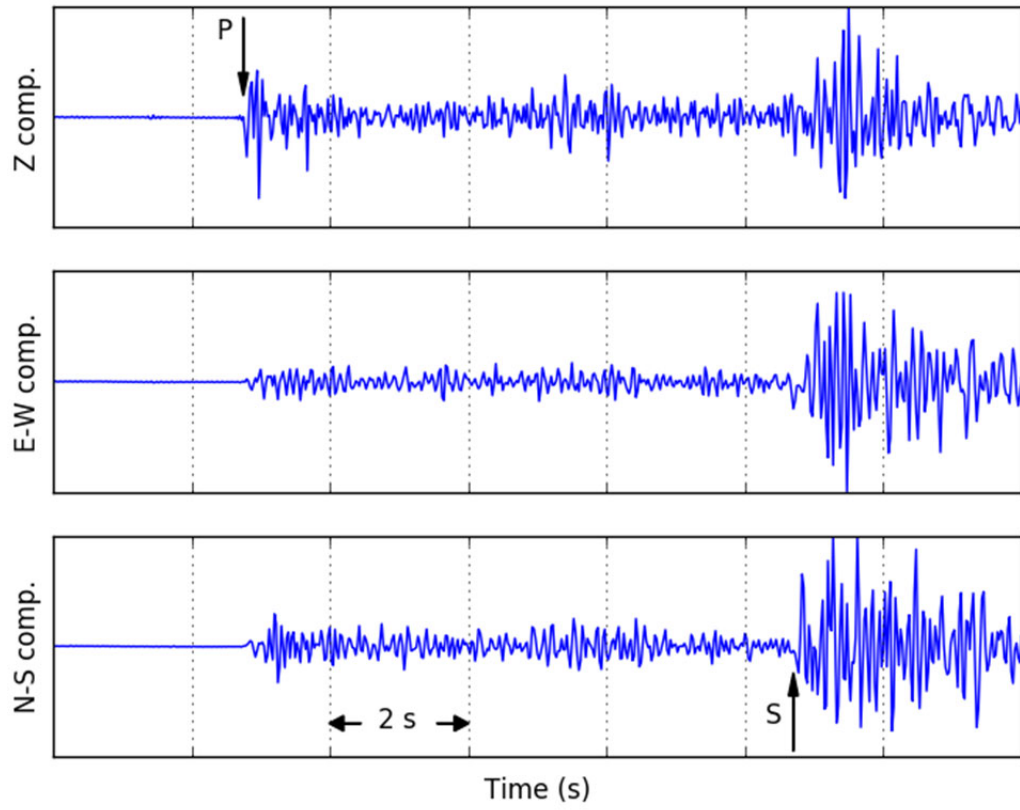
Event: 2001-12-13 08:56:47.46 Station RBSH



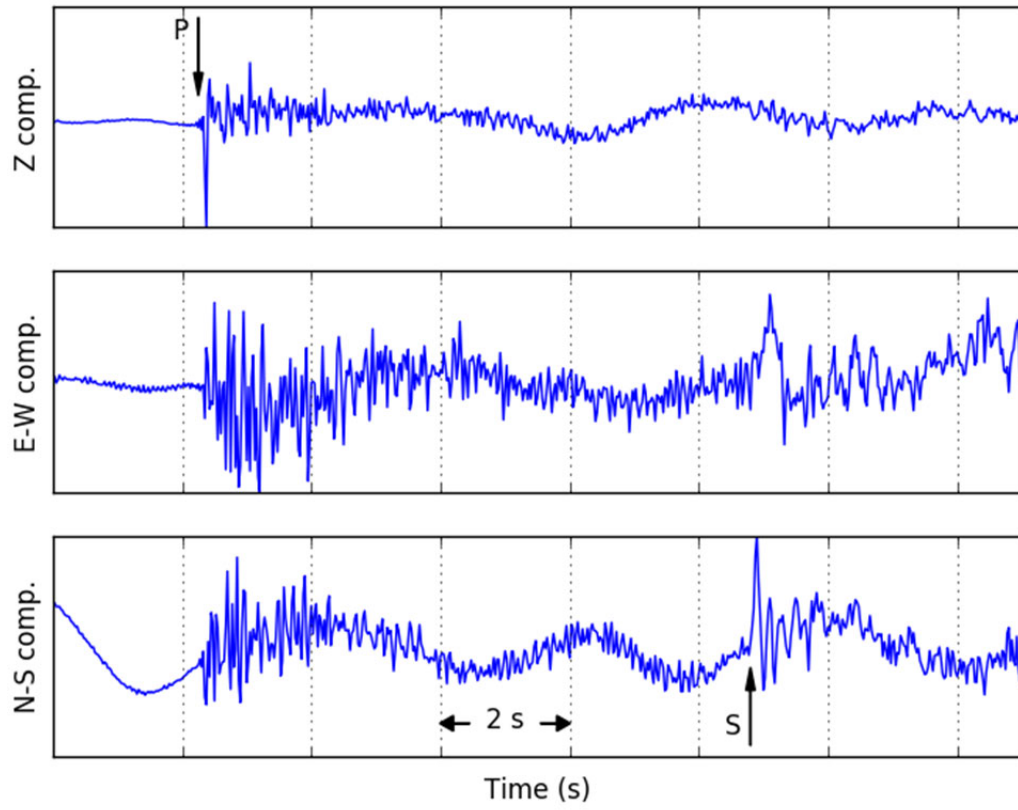
Event: 2002-1-13 14:32:09.62 Station DINX



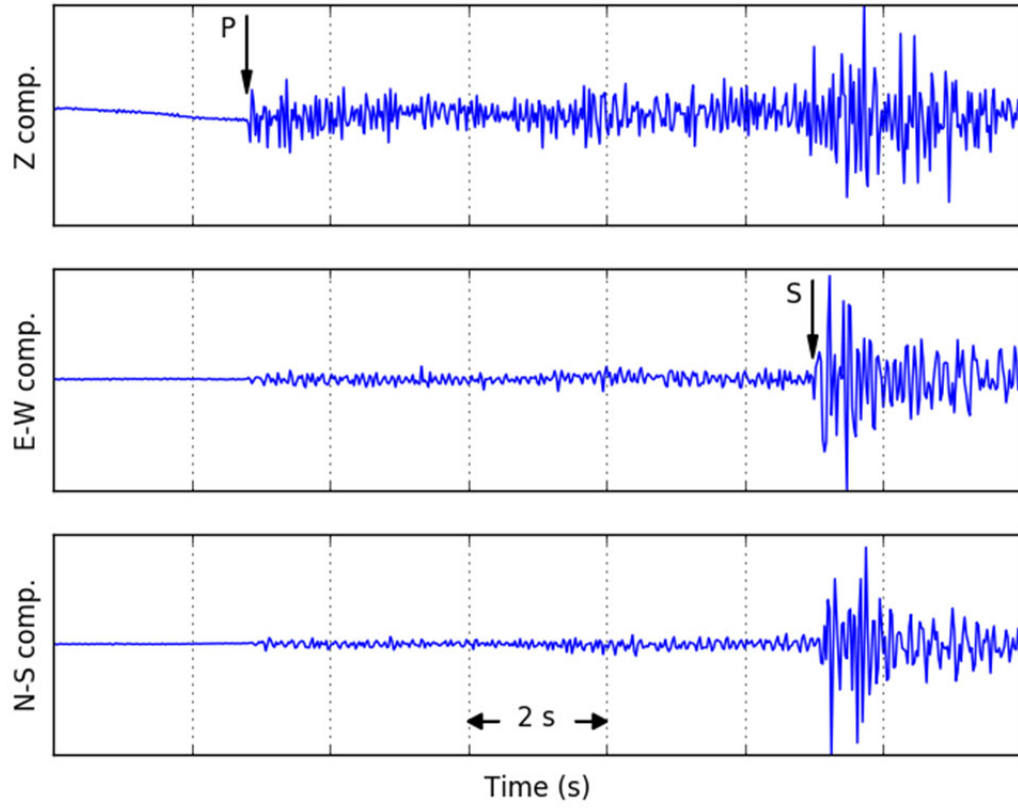
Event: 2002-1-13 14:32:09.62 Station RBSH



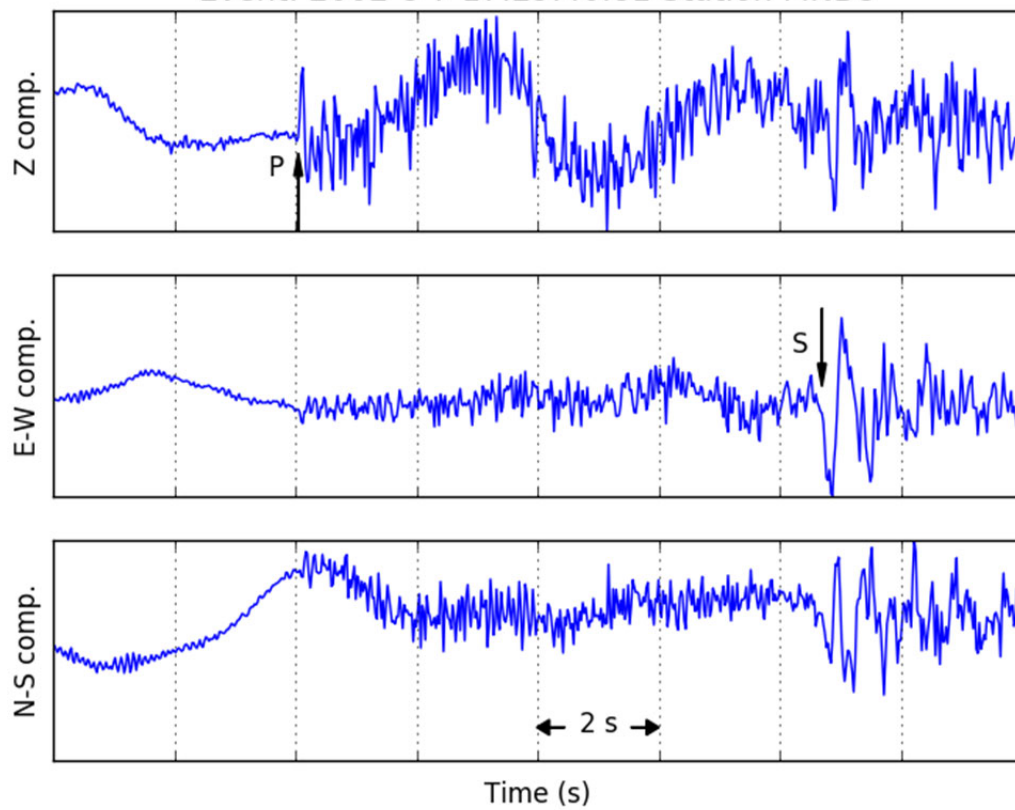
Event: 2002-2-1 15:05:24.06 Station DINX



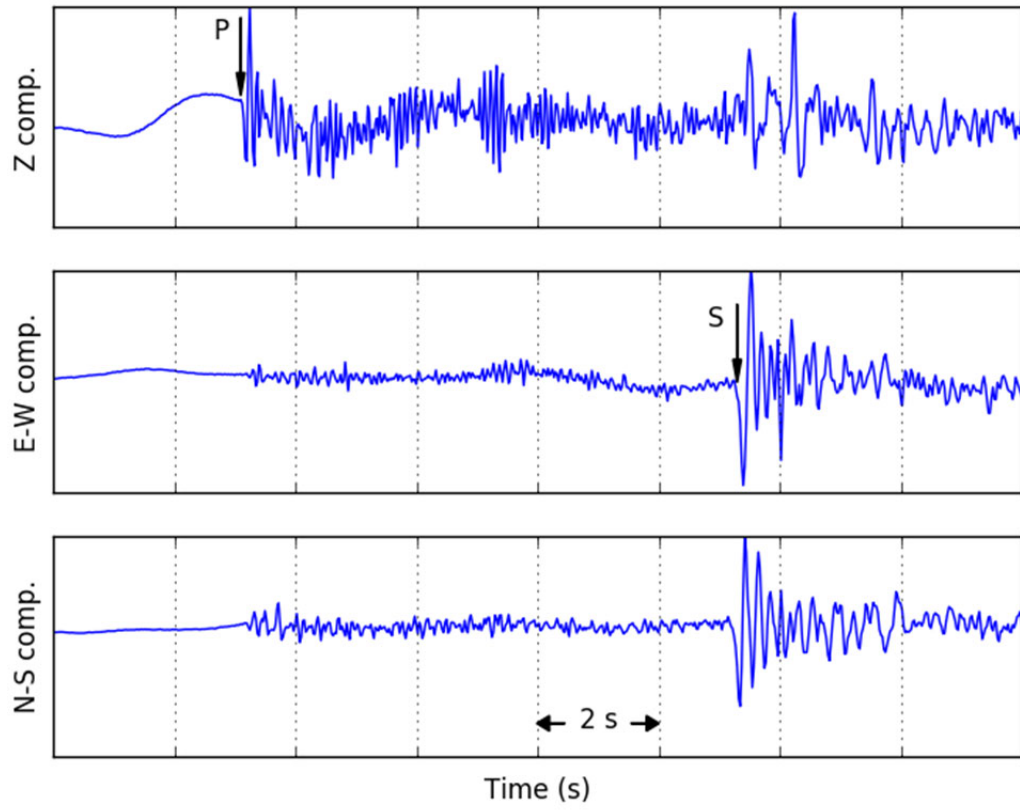
Event: 2002-2-1 15:05:24.06 Station RBSH



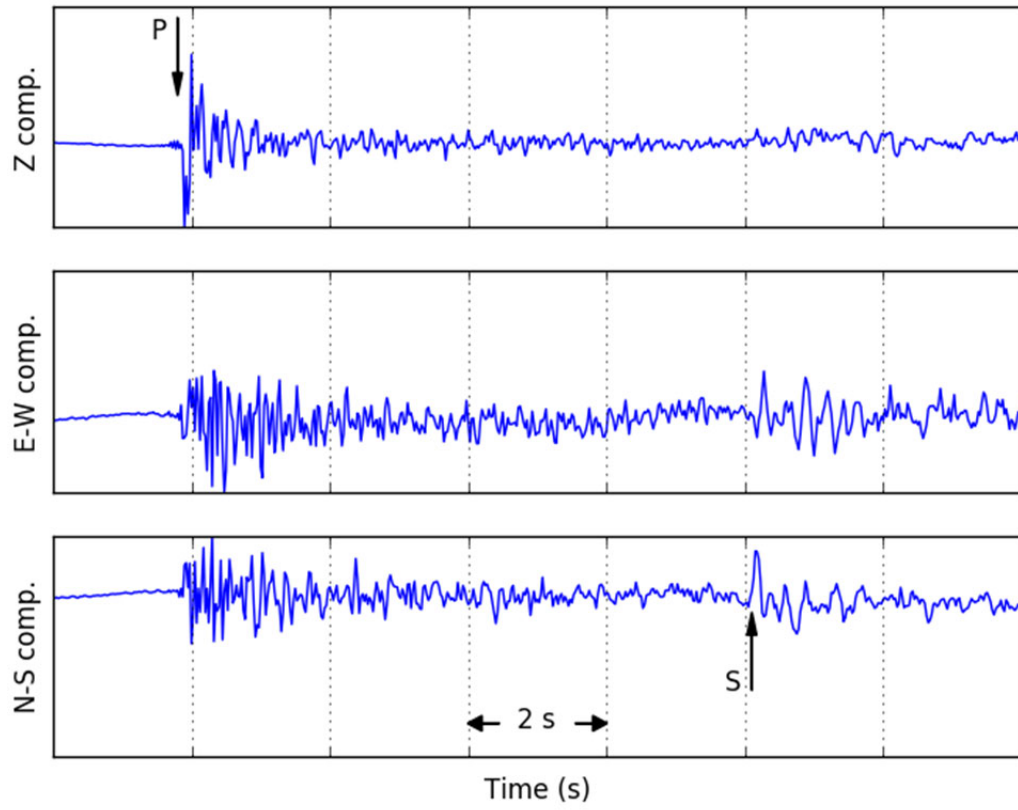
Event: 2002-8-7 17:29:40.81 Station MNBU



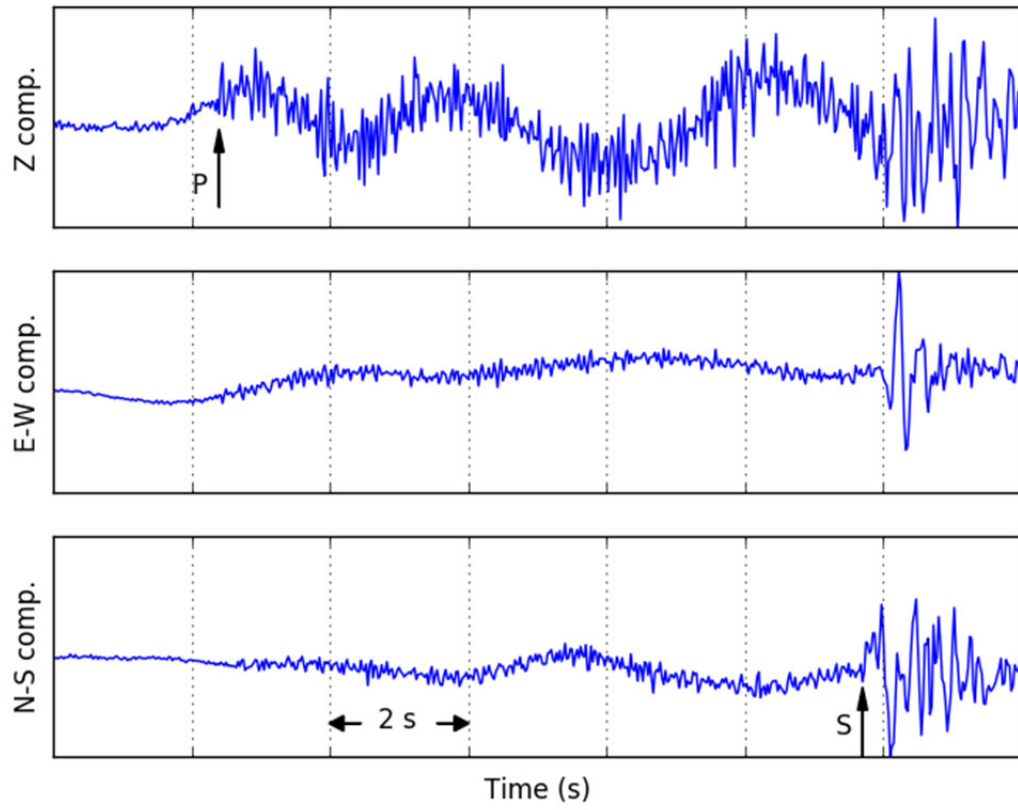
Event: 2002-8-7 17:29:40.81 Station NAIL



Event: 2002-7-19 1:35:35.57 Station DINX



Event: 2002-02-07 05:18:13.21 Station DINX



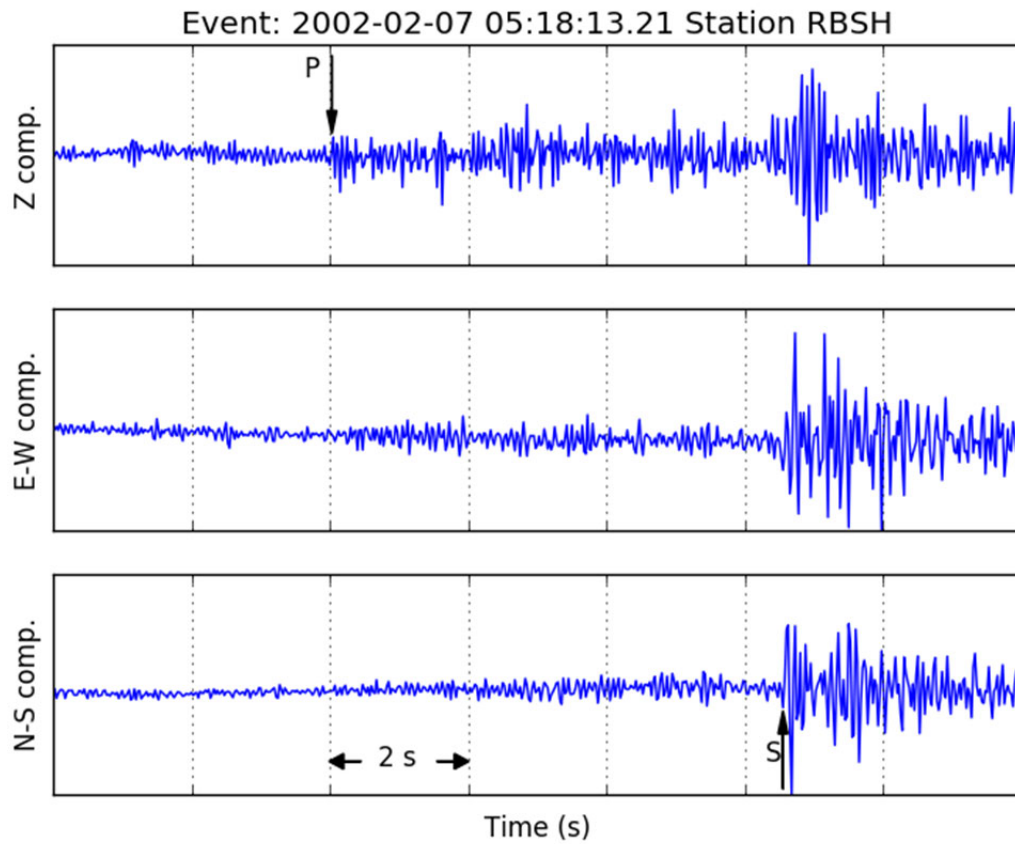


Figure DR4. Raw unfiltered waveforms with P and S picks for the numbered deep events shown in Fig. 2C and Fig. 4. Event 1 occurred on 2001-12-13; Event 2 on 2002-1-13; Event 3 on 2002-2-1; Event 4 on 2002-8-7; Event 5 on 2002-7-19; Event 6 on 2002-02-07.

Table DR1: Parameters for the six numbered events in Fig. 1, 4, and Fig. DR4.

Event number	Latitude (deg)	Longitude (deg)	Depth (km)	Date, Time	Local magnitude
1	28.50	86.87	72.8	2001-12-13 8:56:47.46	N/A
2	28.39	86.77	68.0	2002-1-13 14:32:09.62	2.9
3	28.39	86.94	72.5	2002-2-1 15:5:24.06	2.6
4	28.68	86.50	76.0	2002-8-7 17:29:40.81	2.6
5	28.49	87.24	71.0	2002-7-19 1:35:35.57	2.6
6	28.13	86.85	54.2	2002-02-07 05:18:13.21	2.4

References not cited in main text:

Chen, W.-P. (1988). A Brief Update on the Focal Depths of Intracontinental Earthquakes and their Correlations with Heat Flow and Tectonic Age, *Seismological Research Letters* October 01, 1988, Vol.59, 263-272. doi:10.1785/gssrl.59.4.263.

Chen, W.-P., H. Kao (1996), Seismotectonics of Asia: Some recent progress, in: *The Tectonic Evolution of Asia* A. Yin, M. Harrison, Eds. (Cambridge Univ. Press, Palo Alto) pp. 37-62.

Ekström, G.A. (1987), A Broad Band Method of Earthquake Analysis, Ph. D. thesis, Harvard University.

Lomax, A. (2004), Probabilistic, non-linear, global-search earthquake location in 3D media, Anthony Lomax Scientific Software, Mouans–Sartoux, France.

Utsu, T., Ogata, Y., Matsu'ura, R.S. (1995), The centenary of the Omori formula for a decay law of aftershock activity. *J. Phys. Earth* 43, 1–33. doi:[10.4294/jpe1952.43.1](https://doi.org/10.4294/jpe1952.43.1).

Zhu, L. and Helmberger, D. V. (1996), Intermediate depth earthquakes beneath the India-Tibet collision zone. *Geophysical Research Letters*, 23 (5). pp. 435-438, doi:[10.1029/96GL00385](https://doi.org/10.1029/96GL00385).